Geophys. J. Int. (2005) **161,** 213–229 doi: 10.1111/j.1365-246X.2005.02590.x

Plane waves in viscoelastic anisotropic media—II. Numerical examples

Vlastislav Červený[1] and Ivan Pšenčík[2]

[1]*Department of Geophysics, Faculty of Mathematics and Physics, Charles University, Ke Karlovu* 3, 121 16 *Praha* 2, *Czech Republic. E-mail: vcerveny@seis.karlov.mff.cuni.cz*

[2]*Geophysical Institute, Acad. Sci. of the Czech Republic, Boční II,* 141 31 *Praha* 4, *Czech Republic. E-mail: ip@ig.cas.cz*

Accepted 2005 January 20. Received 2004 December 17; in original form 2004 July 2

SUMMARY

Properties of homogeneous and inhomogeneous plane waves propagating in unbounded viscoelastic anisotropic media in an arbitrarily specified direction are studied numerically. The analytical expressions and algebraic equations of the sixth degree derived in the companion paper (Paper I, this issue) are used for this purpose. Studied characteristics are phase velocity, amplitude decay along the propagation direction, attenuation, attenuation angle and polarization vector. Simple analytical expressions are used to describe the behaviour of *SH* plane waves propagating in a plane of symmetry of a viscoelastic anisotropic medium. Characteristics of *P* and *S* plane waves are determined by solving a complex-valued algebraic equation of the sixth degree. Combined effects of attenuation and anisotropy are illustrated on several models of viscoelastic anisotropic media. The explanation of the so-called forbidden directions known from the directional specification of the slowness vector is given. Non-physical results related to forbidden directions do not arise in the algorithm used.

Key words: polarization, seismic anisotropy, seismic waves, viscoelasticity.

1 INTRODUCTION

Many parts of the Earth's interior display seismic anisotropy and attenuation. Considerable attention has been devoted to wave propagation in elastic anisotropic or dissipative isotropic media. The study of wave propagation in anelastic anisotropic media, however, still deserves attention. Such a study is necessary for correct modelling of seismic wave propagation in anelastic anisotropic media as well as for understanding the phenomena related to such propagation. We concentrate on unbounded viscoelastic anisotropic media specified by a tensor of complex-valued frequency-dependent density-normalized viscoelastic moduli a_{ijkl} whose real part is positive definite and whose imaginary part is zero or negative definite with respect to pairs of indices i, j and k, l. We study several characteristics describing the propagation of a harmonic plane wave with an arbitrarily chosen but fixed positive frequency through such a medium.

For the study, we use the formulae derived in the related paper (Červený & Pšenčík 2005) for the so-called *mixed specification* of the complex-valued slowness vector (are also Červený, 2004)

$$\mathbf{p} = \sigma \mathbf{n} + \mathrm{i} D \mathbf{m}. \tag{1}$$

Here, $\mathbf{n}$ and $\mathbf{m}$ are two mutually perpendicular, real-valued unit vectors, assumed to be known. The vector $\mathbf{n}$ represents a normal to the plane of constant phase, i.e. to the wave front. It may point in the direction of propagation (direction of the real part of the slowness vector $\mathbf{p}$) if the real part of σ is positive or against it if the real part of σ is negative. The vector $\mathbf{m}$ is tangential to the wave front. The vectors $\mathbf{n}$ and $\mathbf{m}$ define the *propagation–attenuation plane* $\Sigma^{\parallel}$, in which the considered complex-valued slowness vector $\mathbf{p}$ is situated. The real-valued quantity D, called the *inhomogeneity parameter*, is also assumed to be known. Its absolute value $|D|$ characterizes inhomogeneity (deviation from homogeneity) of the wave, and it is therefore called the *strength of inhomogeneity*. The complex-valued quantity σ, which represents the projection of the slowness vector $\mathbf{p}$ to the vector $\mathbf{n}$, is a sought quantity. It can be determined from the condition following from the requirement that the plane wave with the slowness vector (1) satisfies the elastodynamic equation. For unrestricted anisotropy and viscoelasticity, the condition for the determination of σ can be expressed in terms of a sixth-degree algebraic equation. Thus the task of finding the slowness vector for given vectors $\mathbf{n}$, $\mathbf{m}$ and an inhomogeneity parameter D in a general viscoelastic anisotropic medium reduces to solving this algebraic equation. An alternative way is to seek σ as the eigenvalues of a 6×6 complex-valued matrix. Here, we use the former approach based on the solution of the algebraic equation. The mixed specification of the slowness vector leads to incomparably simpler algorithms to compute the slowness vectors of plane waves propagating in unbounded anisotropic viscoelastic media than the directional specification commonly used in isotropic viscoelastic media (see a detailed discussion in Červený & Pšenčík 2005). The mixed specification is thus a natural and convenient tool for studying details of plane wave propagation in general unbounded viscoelastic anisotropic media in a specified arbitrary direction of propagation.

We study numerically the behaviour of several characteristics of homogeneous and inhomogeneous plane waves in unbounded

viscoelastic anisotropic media, specifically phase velocity, the imaginary part of the parameter σ (which describes exponential decay of plane wave amplitudes in the direction of propagation), attenuation, attenuation angle and polarization. We have to keep in mind that we study all the mentioned characteristics with respect to the direction of propagation specified by the vector **n** and not with respect to the direction of energy flux. In the latter case, the behaviour of the above-listed characteristics would look different. First we concentrate on *SH* plane waves propagating in a plane of symmetry of a viscoelastic anisotropic medium. Červený & Pšenčík (2005) derived simple analytical expressions for this case which are used for the evaluation of characteristics of *SH* plane waves. Next we study all three waves propagating in anisotropic viscoelastic media. In this case, numerical solution of a sixth-degree algebraic equation is sought. Analysis of the obtained results reveals a series of phenomena unfamiliar from studies of plane wave propagation in elastic anisotropic or viscoelastic isotropic media. The phenomena are discussed in detail in the paper.

In the seismological literature much attention has been devoted to properties of homogeneous and inhomogeneous plane waves propagating in viscoelastic isotropic media (see, for example, Buchen (1971), Borcherdt (1973, 1977), Aki & Richards (1980), Krebes (1983), Richards (1984), Borcherdt & Wennerberg (1985), Borcherdt *et al.* (1986), Caviglia & Morro (1992), Carcione (1993, 2001) and Brokešová & Červený (1998), where many other references can be found). Studies of properties of homogeneous and inhomogeneous plane waves propagating in viscoelastic anisotropic media are not so common. Let us mention here the pioneering studies of *SH* plane waves propagating in a viscoelastic transversely isotropic medium by Krebes & Le (1994) and of *SH* plane waves propagating in a symmetry plane of a monoclinic viscoelastic medium by Carcione & Cavallini (1995, 1997).

In Section 2, basic equations for the mixed specification of a slowness vector are summarized. These equations are used in the computations, the results of which are presented in the following sections. In Section 3, analysis of results obtained for *SH* waves from simple analytical formulae is made. The results for *SH* plane waves propagating in a symmetry plane of a viscoelastic anisotropic medium are compared with results of the same formulae for a viscoelastic isotropic medium. In Section 4, analogous results for all three waves, *P*, *S1* and *S2*, propagating in viscoelastic anisotropic media are analysed. Section 5 contains a detailed explanation of the phenomenon of forbidden directions, and Section 6 offers some concluding remarks.

2 BASIC EQUATIONS

As shown by Červený & Pšenčík (2005), the specification (1) leads to a system of linear equations

$$a_{ijkl}(\sigma n_j + \mathrm{i}Dm_j)(\sigma n_l + \mathrm{i}Dm_l)U_k = U_i, \quad i = 1, 2, 3 \tag{2}$$

for the polarization vector **U** and to the algebraic equation of the sixth degree

$$\det[a_{ijkl}(\sigma n_j + \mathrm{i}Dm_j)(\sigma n_l + \mathrm{i}Dm_l) - \delta_{ik}] = 0 \tag{3}$$

for the quantity σ. In (2) and (3), a_{ijkl} are complex-valued density-normalized viscoelastic moduli specified for a fixed frequency. Eq. (3) is a polynomial equation with coefficients, which are generally complex-valued (for the coefficients, see Fedorov 1968 but note misprints in the coefficients with powers 5 and 2). Eq. (3) has six roots corresponding to *S1*, *S2* and *P* plane waves propagating in the directions of $\pm\mathbf{n}$. Various methods can be used to solve eq. (3). Here we either evaluate an analytical solution of eq. (3) derived by Červený & Pšenčík (2005) for the propagation of *SH* plane waves in a plane of symmetry of a viscoelastic anisotropic medium, or solve eq. (3) numerically, using Laguerre's method (see Press *et al.* 1986).

We consider inhomogeneous plane waves with vectors **n** and **m** confined to the plane (x_1, x_3), i.e. the plane (x_1, x_3) is the propagation–attenuation plane. This means that the components of the vectors **n** and **m** can be expressed as

$$\begin{aligned} &n_1 = \sin i, \quad n_2 = 0, \quad n_3 = \cos i, \\ &m_1 = \cos i, \quad m_2 = 0, \quad m_3 = -\sin i. \end{aligned} \tag{4}$$

Here i is the propagation angle.

The slowness vector **p** can be written alternatively as

$$\mathbf{p} = \mathbf{P} + \mathrm{i}\mathbf{A}, \tag{5}$$

where the real-valued vector **P** is the *propagation vector*, $\mathbf{P} = |\mathbf{P}|\mathbf{N}$, the real-valued vector **A** is the *attenuation vector*, $\mathbf{A} = |\mathbf{A}|\mathbf{M}$, **N** and **M** being real-valued unit vectors. The propagation vector **P** points in the direction of the propagation of the wave front and the attenuation vector **A** is oriented in the direction of the maximum decay of amplitudes. The vectors **N** and **M** make an angle γ called the *attenuation angle*, $\cos\gamma = \mathbf{N}\cdot\mathbf{M}$.

By comparing eqs (5) and (1), we can see that the direction of the propagation vector $\mathbf{P} = \mathrm{Re}\sigma\ \mathbf{n}$ is parallel to the vector **n** and points along or against it depending on the sign of $\mathrm{Re}\sigma$. Therefore, $\mathbf{N} = \pm\mathbf{n}$. The attenuation vector $\mathbf{A} = \mathrm{Im}\sigma\ \mathbf{n} + D\mathbf{m}$ has, in general, projections into **n** and **m**. For $D = 0$ (homogeneous wave), the attenuation vector is parallel to **n** and points along or against it depending on the sign of $\mathrm{Im}\sigma$. For $\mathrm{Im}\sigma = 0$ and $D \neq 0$ (inhomogeneous waves in isotropic elastic media), the attenuation vector is parallel to **m**.

From eq. (5), we get simply the *directional specification* of the slowness vector,

$$\mathbf{p} = \mathcal{C}^{-1}(\mathbf{N} + \mathrm{i}\delta\mathbf{M}). \tag{6}$$

In the directional specification, the vectors **N** and **M** are assumed to be known; thus the attenuation angle γ is also known. The phase velocity $\mathcal{C}$ and the attenuation–propagation ratio δ are the quantities sought. Eq. (6) represents the most common specification of the complex-valued slowness vector in the seismological literature, particularly in isotropic viscoelastic media.

For a value of σ determined by solving eq. (3), the relevant propagation vector **P**, the attenuation vector **A**, unit vectors **N** and **M**, phase velocity $\mathcal{C}$, the attenuation–propagation ratio δ and the attenuation angle γ related to the inhomogeneous plane wave under consideration can be determined from the formulae (Červený & Pšenčík 2005):

$$\begin{aligned} P_1 &= n_1(\mathrm{Re}\sigma), \\ P_3 &= n_3(\mathrm{Re}\sigma) \\ A_1 &= n_1(\mathrm{Im}\sigma) + n_3 D, \\ A_3 &= n_3(\mathrm{Im}\sigma) - n_1 D, \\ |\mathbf{P}| &= |\mathrm{Re}\sigma|, \\ |\mathbf{A}| &= [(\mathrm{Im}\sigma)^2 + D^2]^{1/2}, \\ N_1 &= \epsilon n_1, \\ N_3 &= \epsilon n_3, \\ M_1 &= [n_1(\mathrm{Im}\sigma) + n_3 D]/[(\mathrm{Im}\sigma)^2 + D^2]^{1/2}, \\ M_3 &= [n_3(\mathrm{Im}\sigma) - n_1 D]/[(\mathrm{Im}\sigma)^2 + D^2]^{1/2}, \\ \mathcal{C} &= 1/|\mathrm{Re}\sigma|, \\ \delta &= [(\mathrm{Im}\sigma)^2 + D^2]^{1/2}/|\mathrm{Re}\sigma|, \\ \cos\gamma &= \epsilon\mathrm{Im}\sigma/[(\mathrm{Im}\sigma)^2 + D^2]^{1/2}. \end{aligned} \tag{7}$$

Here, ϵ is given by

$$\epsilon = \mathrm{Re}\sigma/|\mathrm{Re}\sigma| = \pm 1. \tag{8}$$

In the propagation–attenuation plane $\Sigma^{\parallel}$, which is identical with the plane (x_1, x_3), $P_2 = A_2 = N_2 = M_2 = 0$.

In the following, we study properties of inhomogeneous plane waves in the propagation–attenuation plane $\Sigma^{\parallel}$. In this plane, the waves are specified by two parameters: the propagation angle i and the inhomogeneity parameter D. Two types of pictures are presented: (i) For i fixed, considering variation of the inhomogeneity parameter D. (ii) For D fixed, considering variation of the propagation angle i (polar graphs). In the figures the phase velocity $\mathcal{C}$ is measured in km s^{-1}, the quantity σ, the attenuation $|\mathbf{A}|$ and inhomogeneity parameter D in (s km)$^{-1}$, and the propagation angle i and the attenuation angle γ in degrees. The frequency is kept constant in all studies.

3 *SH* PLANE WAVES IN A SYMMETRY PLANE

In this section, we discuss the properties of inhomogeneous and homogeneous *SH* plane waves, propagating in the plane of symmetry Σ^S of a monoclinic anisotropic viscoelastic medium. We assume that Σ^S is identical with the propagation–attenuation plane $\Sigma^{\parallel}$, and both planes coincide with the plane (x_1, x_3). As shown in eq. (57) of Červený & Pšenčík (2005), eq. (3) has two simple analytical solutions in this case:

$$\sigma_{1,2} = -\mathrm{i}D\Lambda\Gamma_{22}^{-1} \pm \left(\Gamma_{22}^{-1} + D^2\Gamma_{22}^{-2}\Delta\right)^{1/2}, \tag{9}$$

where

$$\begin{aligned} \Gamma_{22} &= A_{66}n_1^2 + A_{44}n_3^2 + 2A_{46}n_1n_3, \\ \Lambda &= (A_{66} - A_{44})n_1n_3 + A_{46}\left(n_3^2 - n_1^2\right), \\ \Delta &= A_{44}A_{66} - A_{46}^2, \end{aligned} \tag{10}$$

and D is the inhomogeneity parameter. The quantities A_{44}, A_{46} and A_{66} are the density-normalized viscoelastic moduli in the Voigt notation. The two values of σ correspond to the two *SH* waves propagating in the directions of $\pm\mathbf{n}$.

The model of viscoelastic anisotropic medium used is close to that used by Carcione & Cavallini (1995) in the computations based on the directional specification of the slowness vector of an *SH* wave. The density-normalized viscoelastic moduli are:

$$A_{44} = 5 - \mathrm{i}, \quad A_{66} = 11.25 - 1.125\mathrm{i}, \quad A_{46} = 2.5. \tag{11}$$

All quantities in (11) have dimensions (km^2 s^{-2}). Both anisotropy and dissipation considered in (11) are rather strong. We therefore also present additional results for models closer to isotropy and perfect elasticity.

3.1 *SH* plane waves in isotropic viscoelastic media: variations with D

To study the combined effects of anisotropy and viscoelasticity on plane waves it is useful to start with some reference results for isotropic viscoelastic media. The properties of plane waves in isotropic viscoelastic media have been extensively studied in the seismological literature (for a list of selected references see Červený & Pšenčík 2005). In most of the studies the attenuation angle γ was used as a basic parameter specifying slowness vectors of inhomogeneous plane waves. Here, as in the whole text, we consider the mixed specification of the slowness vector, and use the inhomogeneity parameter D as a basic parameter.

For isotropic viscoelastic media the equation for $\sigma_{1,2}$ follows from eqs (9) and (10), if we take into account that $A_{44} = A_{66}$ and $A_{46} = 0$. We then obtain a very simple expression

$$\sigma_{1,2} = \pm(1/\beta^2 + D^2)^{1/2}. \tag{12}$$

Here β is the complex-valued *S*-wave velocity, $\beta^2 = A_{44}$, which is independent of the propagation angle i. Thus, the values $\sigma_{1,2}$ are also independent of the propagation angle. Eq. (12) is valid generally for homogeneous and inhomogeneous plane waves propagating in viscoelastic and perfectly elastic media. It even holds for *P* waves, if we substitute the *S*-wave velocity β by the *P*-wave velocity α. Inserting (12) into (7), we can evaluate various characteristics of *S* waves propagating in isotropic viscoelastic media.

Let us illustrate behaviour of some of the quantities listed in (7) in viscoelastic isotropic models close to the anisotropic viscoelastic model (11). The models are obtained by varying the imaginary part of the square of the *S*-wave velocity:

$$\beta^2 = 5 - \mathrm{i}\nu. \tag{13}$$

In (13), we consider the following values of ν: $\nu = 1$, 0.5, 0.25 and 0. If we express β^2 in terms of the real-valued *S*-wave velocity V_S and the quality factor Q_S, so that $\beta^2 = V_S^2(1 - \mathrm{i}/Q_S)$, we obtain $V_S^2 = 5$ and $Q_S = 5$, 10, 20 and ∞, respectively.

In the following, we study the behaviour of selected characteristics of *SH* plane waves in isotropic media as functions of the inhomogeneity parameter D. The results are independent of the propagation angle i. Fig.1 displays the variations of $\mathcal{C}$, Imσ, $|\mathbf{A}|$ and γ with D, $D \in (-0.2, 0.2)$. Each frame of Fig. 1 shows black, red, green and blue curves corresponding to (13) with $\nu = 1$, 0.5, 0.25 and 0, respectively. Let us list the most important observations:

(1) All curves are *symmetric* with respect to $D = 0$, which corresponds to a homogeneous plane wave.

(2) The *phase velocities* $\mathcal{C}$ depend only slightly on the value of Q_S, for D fixed. For example, for $D = 0$, they increase from 2.236 km s^{-1} for the perfectly elastic case ($Q_S = \infty$, blue) to 2.269 km s^{-1} for $Q_S = 5$ (black). However, they change more strongly with increasing inhomogeneity strength $|D|$. The maximum phase velocity is always obtained for the homogeneous plane wave ($D = 0$). It follows from (7) and (12) that $\mathcal{C} \to 0$ for $|D| \to \infty$.

(3) The *values* of Imσ controlling the amplitude decay along the propagation vector **P** are zero for perfectly elastic isotropic medium (blue) and positive for an viscoelastic isotropic medium. This means that the exponential decay of amplitudes is always positive along the direction of propagation in isotropic viscoelastic media. The values of Imσ depend considerably on the dissipative properties of the medium; they increase considerably with decreasing value of the quality factor Q_S. Imσ is practically independent of D, at least for small D. Only for strongly dissipative media does Imσ slightly decrease with increasing $|D|$. Note that the zero value of Imσ for a perfectly elastic isotropic medium does not mean that inhomogeneous plane waves do not propagate in perfectly elastic media. Zero Imσ only indicates that there is no exponential decay in the direction **n**. As $\mathbf{p} = \sigma\mathbf{n} + \mathrm{i}D\mathbf{m}$, the exponential decay of an inhomogeneous plane wave propagating in an elastic isotropic medium is always in the direction **m**. This means that homogeneous plane waves do not exist in perfectly elastic media.

(4) The *attenuation* $|\mathbf{A}|$ has a hyperbolic form for varying D, with a minimum for $D = 0$ (homogeneous plane waves). With the exception of very small $|D|$, it increases approximately linearly with $|D|$, and depends only slightly on the quality factor Q_S. For perfectly elastic media, eqs (7) and (12) yield exactly $|\mathbf{A}| = |D|$.

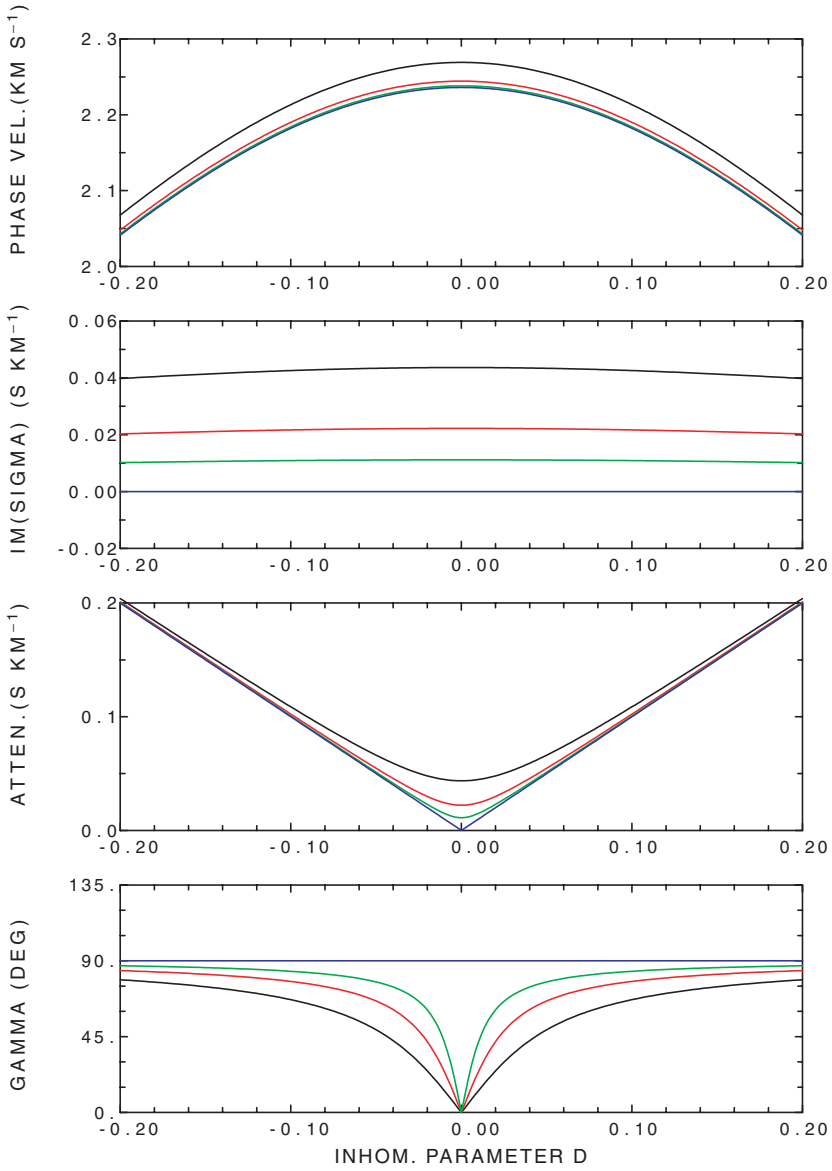

Figure 1. Variations with D of the phase velocity $\mathcal{C}$, Imσ, the attenuation $|\mathbf{A}|$ and the attenuation angle γ of *SH* plane waves in a viscoelastic isotropic model (13). Colours correspond to varying values of ν in (13): $\nu = 1$ (black), $\nu = 0.5$ (red), $\nu = 0.25$ (green) and $\nu = 0$ (blue; a perfectly elastic isotropic medium).

(5) The most interesting results are obtained for the *attenuation angle* γ. It is well known from classical studies that the attenuation angle in isotropic, perfectly elastic or viscoelastic media never exceeds 90°. For a perfectly elastic isotropic medium (blue curve), the attenuation angle γ always equals 90°. The behaviour of γ in viscoelastic isotropic media with respect to D is very interesting for small D. For $D = 0$ (homogeneous plane waves), γ is zero. The value of γ, however, increases very fast with increasing $|D|$, and for $|D| \to \infty$, it approaches 90°. The increase is faster and more concentrated to small $|D|$ for increasing values of the quality factor Q_S.

Let us emphasize that the value of σ varies very slowly with D for small values of $|D|$ (see plots for $\mathcal{C} = 1/|\mathrm{Re}\sigma|$ and Imσ). Thus, the expression (12) for σ can be simply used in the perturbation methods, particularly for weakly dissipative media. Eq. (12) can also be expanded to yield approximate linear or quadratic expressions for σ in terms of D. This is impossible if we use a directional specification of the slowness vector in terms of the attenuation angle γ. Specifically for $|D|$ small and for weakly dissipative media, the attenuation angle γ is varying extremely fast. In fact, this is well known from classical studies, in which the expressions for the slowness vector contain the product $Q_S \cos\gamma$ (see, for example, eq. 5.96 of Aki & Richards 1980). In the limiting case of perfectly elastic media this product is indefinite (as $Q_S = \infty$, $\gamma = 90°$). Thus for weakly dissipative media, which are the main object of our interest, $Q_S \cos\gamma$ is very unstable. All these difficulties are removed by considering the mixed specification of the slowness vector and using the inhomogeneity parameter D instead of γ.

3.2 *SH* plane waves in a symmetry plane of anisotropic viscoelastic media: variations with *D*

In this section we discuss numerical results describing properties of *SH* plane waves, propagating in the plane of symmetry Σ^S

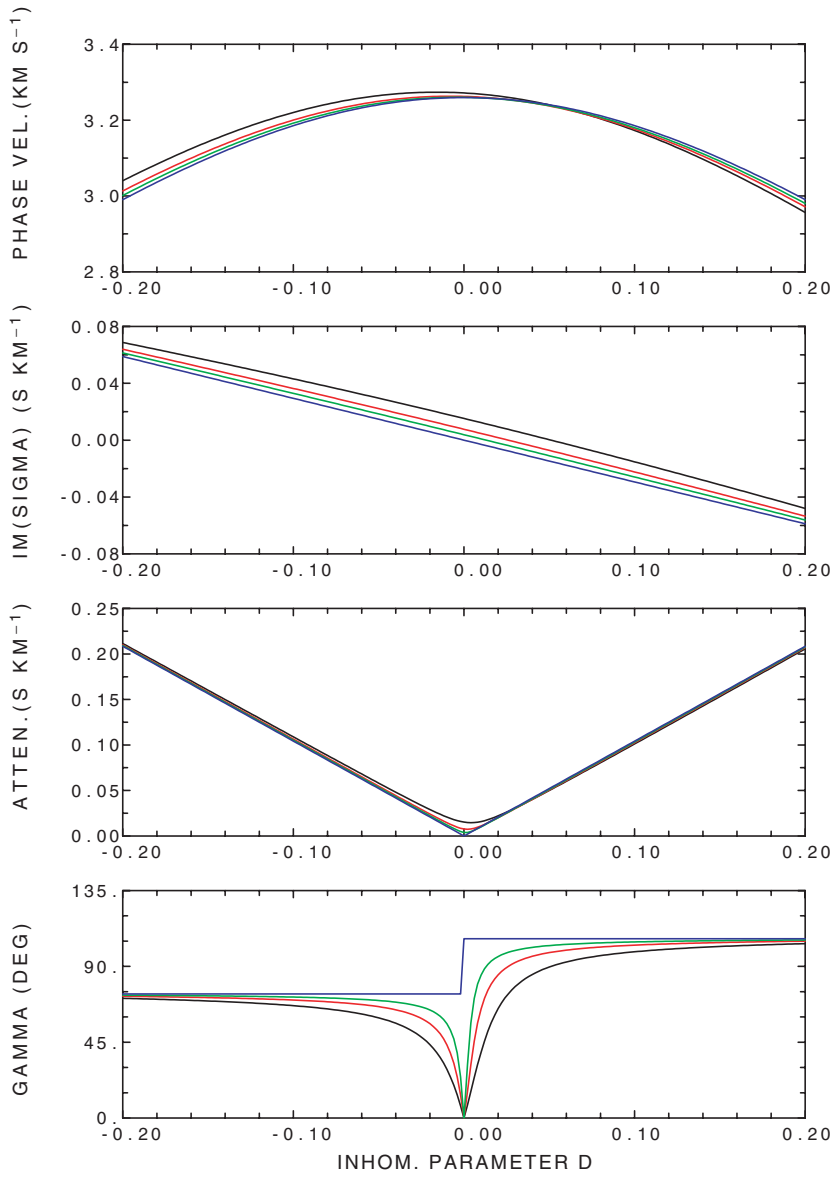

Figure 2. Variations with D of the phase velocity $\mathcal{C}$, Imσ, the attenuation $|\mathbf{A}|$ and the attenuation angle γ of *SH* plane waves in the medium (11) (black), the medium (11) with the twice and four times smaller imaginary parts (red and green, respectively), and to the medium (11) with zero imaginary parts of viscoelastic moduli (blue; perfectly elastic medium). The propagation angle $i = 45^\circ$.

of a monoclinic anisotropic viscoelastic medium. Let us emphasize that propagation of *SH* plane waves in symmetry planes of transversely isotropic and monoclinic viscoelastic media has been studied by Krebes & Le (1994) and Carcione & Cavallini (1995), respectively. They used the directional specification of the slowness vector. As in Section 3.1, we study here various characteristics of homogeneous and inhomogeneous plane waves as functions of the inhomogeneity parameter D, with the propagation angle i fixed.

As the reference viscoelastic anisotropic model, we consider model specified by the density-normalized complex-valued viscoelastic moduli A_{44}, A_{66} and A_{46}, given by (11). In Figs 2 and 3, results corresponding to the model (11) are denoted by black curves. The red and green curves correspond to the twice and four times smaller imaginary parts in (11), and the blue curve corresponds to the relevant perfectly elastic anisotropic medium. Specifically, the values of ImA_{44}, ImA_{66}, and ImA_{46} are successively -1, -1.125, 0 (black), -0.5, -0.5625, 0 (red), -0.25, -0.28125, 0 (green) and 0, 0, 0 (blue). The propagation angle i equals 45° in Fig. 2 and 135° in Fig. 3. Let us first discuss Fig. 2, corresponding to the propagation angle $i = 45^\circ$, and let us list the most important observations:

(1) All curves plotted in Fig. 2 are, in contrast to Fig. 1, *non-symmetric* with respect to $D = 0$.

(2) The behaviour of *phase velocities* in anisotropic viscoelastic media has some features similar to those in isotropic viscoelastic media. The phase velocities depend only slightly on the dissipative parameters of the media. For example, for homogeneous plane waves ($D = 0$), the phase velocities for the four models are respectively 3.27178, 3.26265, 3.26036 and 3.25960 km s^{-1}. For $|D| \to \infty$, the phase velocities decrease to zero. There are, however, certain differences between the behaviour of phase velocities in isotropic and anisotropic viscoelastic media: phase velocities $\mathcal{C}$ in viscoelastic anisotropic media do not attain their maximum value $\mathcal{C}^M$ for

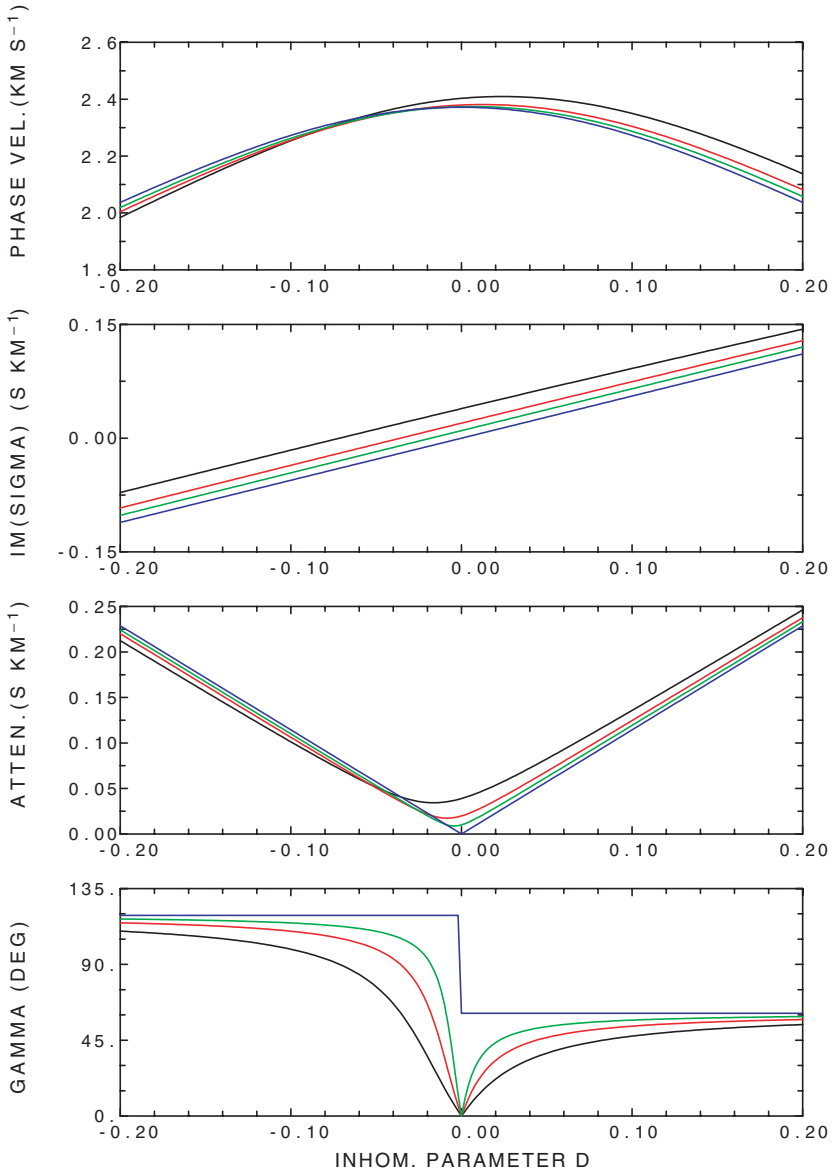

Figure 3. The same as in Fig. 2 but for the propagation angle $i = 135^\circ$.

$D = 0$ (homogeneous plane wave) as in isotropic viscoelastic media, but for $D = D^M \neq 0$ (inhomogeneous plane wave). The shift of the maximum phase velocity from $D = 0$ to $D = D^M$ is small but observable (see Fig. 2). Approximate analytical expressions for D^M and $\mathcal{C}^M$ are given in eqs (68–69) of Červený & Pšenčík (2005). If we take into account that the phase velocity of the homogeneous plane wave $\mathcal{C}_{hom}$ equals $1/a$, we obtain $\mathcal{C}^M - \mathcal{C}_{hom} \doteq b^2/4ca^2 > 0$. For a, b and c, see (67) of Červený & Pšenčík (2005). We can also see that for negative values of D the highest phase velocities are in the most attenuating model (black) while for positive values of D the highest phase velocities are in the perfectly elastic model (blue). We give several quantitative results related to D^M and $\mathcal{C}^M - \mathcal{C}_{\rm hom}$ for the models under consideration. For the black curve, $D^M = -0.0160$, $\mathcal{C}^M - \mathcal{C}_{\rm hom} = 0.001995\,{\rm kms}^{-1}$, for the red curve $D^M = -0.0080$ and $\mathcal{C}^M - \mathcal{C}_{\rm hom} = 0.000506\,{\rm kms}^{-1}$ and for the green curve $D^M = -0.0040$ and $\mathcal{C}^M - \mathcal{C}_{\rm hom} = 0.000127\,{\rm kms}^{-1}$. It is not difficult to verify that the approximate relations (68) and (69) of Červený & Pšenčík (2005) give approximately the same results.

(3) There is a great difference between the behaviour of Imσ for viscoelastic isotropic and viscoelastic anisotropic media. For isotropic media, Imσ is always non-negative, and depends only very slightly on D, but strongly on dissipative parameters. For anisotropic viscoelastic media, however, it varies roughly linearly with D for small $|D|$. For $D < D_0$, Imσ is positive, and for $D > D_0$ it is negative. Dependence on dissipative parameters is much weaker. For small $|D|$, a simple approximate analytical relation (70) of Červený & Pšenčík (2005) holds for $D = D_0$, for which Im$\sigma = 0$. For the models used in Fig. 2, and for the propagation angle $i = 45^\circ$, the factor $\Lambda\,\Gamma_{22}^{-1}$ in eq. (9) is positive and Imσ thus decreases with increasing D. We obtain $D_0 = 0.0511$ for the black, $D_0 = 0.02580$ for the red and $D_0 = 0.0131$ for the green curve. For perfectly elastic case (blue), $D_0 = 0$, as simply follows from inspection of eq. (9). The positive value of Imσ has a standard meaning: the amplitudes of inhomogeneous plane waves decay exponentially in the direction of the vector **N**. The existence of negative Imσ (for $D > D_0$) means exponential *growth* of amplitudes in the direction of propagation **N**

for $D > D_0$. An analogous apparent paradox has been discovered in the studies of inhomogeneous *SH* plane waves, based on the directional specification (6) of the slowness vector (with fixed γ) (see Krebes & Le (1994), Carcione & Cavallini (1995) and Carcione (2001)). Physical explanation consists in the fact that the inhomogeneous plane waves always decay exponentially in the direction of the energy flux, which generally differs from the direction of the wave propagation (**N**) in viscoelastic anisotropic media. Here we do not discuss the energy flux of inhomogeneous plane waves, but specify quantitatively the values of inhomogeneity parameter D_0 which separates regions of amplitude growth and decay along the propagation vector.

(4) Behaviour of the *attenuation* $|\mathbf{A}|$ for fixed i and D varying, is not very different for isotropic and anisotropic viscoelastic media (compare Figs 1 and 2). In a similar way as in isotropic viscoelastic media, the curves have a hyperbolic form. With the exception of very small $|D|$, the curves increase approximately linearly with increasing $|D|$. There is, however, one small but remarkable difference. In anisotropic viscoelastic media, the minima $A_{\min}$ of the attenuation curves are not situated at $D = 0$ (homogeneous waves) but at $D = D_{\text{att}} \neq 0$ (inhomogeneous waves). This was predicted in eq. (71) of Červený & Pšenčík (2005). The shift is small, but it is clearly observable in Fig. 2. Let us present numerical values corresponding to the models under consideration. For the blue curve (perfect elasticity) $D_{\text{att}} = 0$ with $A_{\min} = 0$, for the black curve $D_{\text{att}} = 0.0041$ with $A_{\min} = 0.0146$, for the red curve $D_{\text{att}} = 0.0021$ with $A_{\min} = 0.0073$, and for the green curve $D_{\text{att}} = 0.0010$ with $A_{\min} = 0.0036$. This effect might be more expressive for other propagation angles i (see, for example, Fig. 3). Let us note that for perfectly elastic media, eqs (7) and (9) yield $|\mathbf{A}| = |D|(1 + \Lambda^2\, \Gamma_{22}^{-2})^{1/2}$.

(5) Certain properties of the *attenuation angle* γ of *SH* waves in anisotropic viscoelastic media remain similar to those in isotropic viscoelastic media. For $D = 0$, the attenuation angle γ is zero, and increases rapidly with $|D|$ increasing. For $|D| \to \infty$, the attenuation angle γ reaches its boundary values γ^*. The increase of γ with increasing $|D|$ is particularly fast for small $|D|$ in weakly dissipative media. In certain other aspects, the properties of the attenuation angle γ are very different in isotropic and anisotropic viscoelastic media. Let us discuss briefly the most important differences in the behaviour of γ by comparing Figs 1 and 2.

The values of γ in Fig. 2 are not symmetrical with respect to $D = 0$, $\gamma(D) \neq \gamma(-D)$. Consequently, the boundary values γ^* (for infinite $|D|$) are different for $D \to \infty$ and $D \to -\infty$. The values of boundary attenuation angle γ^* are different from 90°. As a rule, γ^* exceeds 90° for one sign of D and is less than 90° for the other sign of D.

Let us present values of boundary attenuation angles γ^* corresponding to the four models used in Fig. 2. For $D > 0$, the values of γ^* are 108.60°, 107.55°, 106.98° and 106.39° (for the elastic case). For $D < 0$, they are: 76.13°, 74.85°, 74.22° and 73.61° (for the elastic case). As we can see, the boundary attenuation angles γ^* for viscoelastic anisotropic media are very close to the attenuation angles for relevant perfectly elastic anisotropic media. In the case of the model (11) the difference does not exceed 2.6°, even though the model (11) is strongly dissipative and strongly anisotropic. The value of γ for perfectly elastic anisotropic media is discontinuous at $D = 0$. It has different constant values for $D > 0$ and for $D < 0$, which are symmetric with respect to 90° as follows from (7) and (9). The values are the same and equal to 90° only when $\Lambda = 0$, i.e. when $(A_{66} - A_{44}) \sin 2i + 2\, A_{46} \cos 2i = 0$. For all other propagation angles i, the attenuation angle γ is different from 90° although it may be close to it (for small Λ). It depends on i and on the sign of D. This result differs from the result obtained for inhomogeneous plane waves propagating in perfectly elastic isotropic media, where the attenuation angle γ always equals 90° and is independent of i.

The attenuation angle γ is closely related to the quantity $\text{Im}\sigma$ (see the last equation of 7). Actually, γ is less than 90° when $\text{Im}\sigma > 0$, equals 90° when $\text{Im}\sigma = 0$ and is greater than 90° when $\text{Im}\sigma < 0$. Thus, the quantity D_0 discussed under point (3) also plays an important role in the discussion of the attenuation angle γ. If we change the inhomogeneity parameter from $D = 0$ to $D = D_0$, the attenuation angle γ changes from 0° to 90°.

In Fig. 2, the propagation angle i equals 45°. Specific behaviour of individual curves remains qualitatively similar to those displayed in Fig. 2 also for other propagation angles i, but may differ in detail. Fig. 3 shows the same curves for the same model as Fig. 2; only the propagation angle i is changed from 45° to 135°. The most distinct differences between Figs 2 and 3 are as follows:

(a) The maximum values $\mathcal{C}^M$ of the phase velocity are shifted from the region $D < 0$ to the region $D > 0$.

(b) The minimum values $A_{\min}$ of the attenuation curves are shifted from the region $D > 0$ to the region $D < 0$, and the difference between individual curves is greater.

(c) The quantity $\text{Im}\sigma$ increases with increasing D, and is zero for $D = D_0 < 0$.

(d) Consequently, $\gamma(-D) > \gamma(D)$ for $D > 0$ in this case.

(e) For a perfectly elastic anisotropic medium, $\gamma = 60.95°$ for $D > 0$, $\gamma = 119.05°$ for $D < 0$. Thus, the deviation of γ from 90° corresponding to the perfectly elastic isotropic case is nearly 30°. Otherwise, all the conclusions made for Fig. 2 remain valid.

The attenuation angle γ is closely related to the so-called forbidden directions (see discussion in Section 5).

3.3 *SH* plane waves in a symmetry plane of anisotropic viscoelastic media: variations with the propagation angle *i*

Here we discuss the properties of *SH* plane waves as functions of the propagation angle i for selected values of the inhomogeneity parameter D. We use the polar graphs, with $i = 0°$ upwards and $i = 90°$ to the right (see eq. 4). In all cases, the presented polar graphs display the absolute values of the relevant quantities (the signs of these quantities are not distinguished). Instead of the attenuation angle γ, we present $\cos\gamma$. If the quantity $\cos\gamma$ passes through the centre of the polar graph, the relevant value of γ passes through 90°. Moreover, the quantity $\text{Im}\sigma$ also passes through the centre of the polar graph in this case.

Fig. 4 shows the polar graphs for the same models as those used in Fig. 2, for $D = 0.02$. We remind the reader that the black curve corresponds to the model (11), the red and green curves to the twice and four times lower dissipation, and the blue curve to the relevant perfectly elastic anisotropic medium.

The polar graphs of the phase velocity $\mathcal{C}$ and of the attenuation $|\mathbf{A}|$ are quite smooth, and never pass through the centre of the graph. The polar graphs for $\text{Im}\sigma$ and $\cos\gamma$ are more complicated. In perfectly elastic media (blue) and in weakly dissipative media (green curves) the curves have four lobes. The polar graphs for $\cos\gamma$ and $\text{Im}\sigma$ are similar in shape in this case. A simple explanation for this similarity follows from the last equation of (7), which yields $\cos\gamma \doteq \epsilon\, \text{Im}\sigma / |D|$ for $(\text{Im}\sigma)^2 \ll D^2$. For a perfectly elastic medium (blue) the shapes of the curves for $\text{Im}\sigma$ and $\cos\gamma$ are practically identical, the scaling factor being the value of D, $D = 0.02$. The propagation

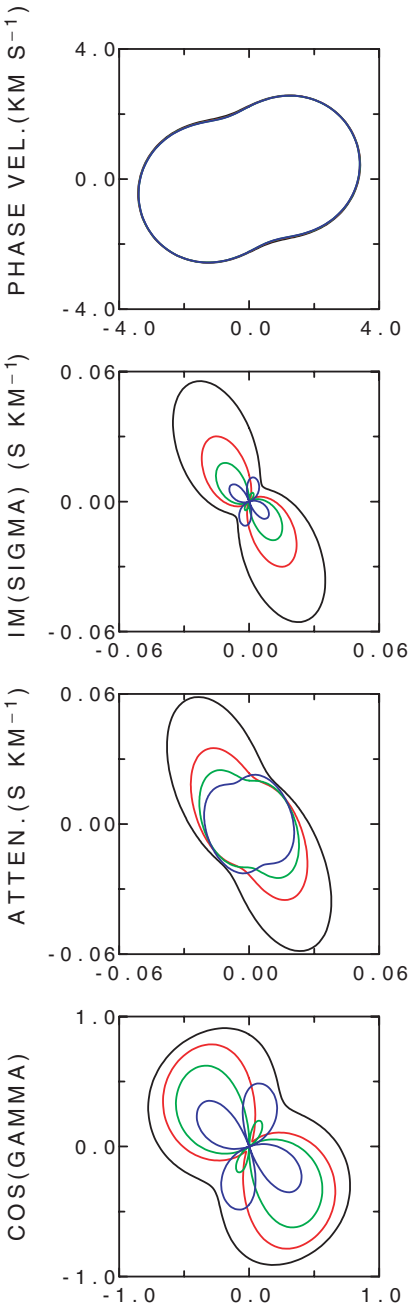

Figure 4. The same as in Fig. 2 but in polar diagrams for the inhomogeneity parameter $D = 0.02$.

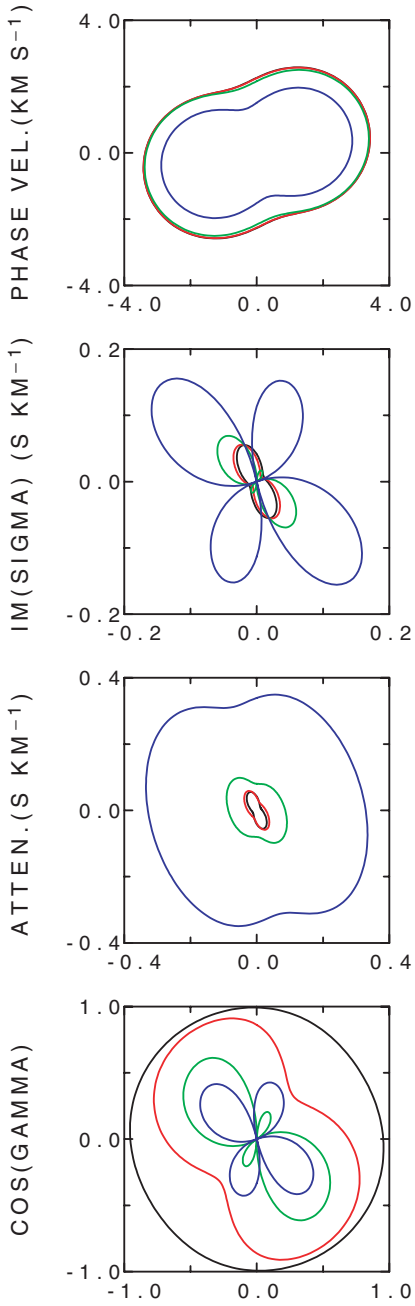

Figure 5. The same as in Fig. 4 but for the model (11) only. Varying inhomogeneity parameters D: $D = 0.005$, black; $D = 0.02$, red; $D = 0.08$, green; $D = 0.32$, blue.

angles i specifying the boundaries between the lobes correspond to zero values of $\cos\gamma$, i.e. to $\gamma = 90^\circ$. Consequently, the neighbouring lobes correspond to the attenuation angles $\gamma < 90^\circ$ and $\gamma > 90^\circ$.

In Fig. 5, the model (11) is considered and the inhomogeneity parameter D is varied, from $D = 0.005$ (black), to 0.02 (red), 0.08 (green) and 0.32 (blue). The red curves in Fig. 5 thus correspond to black curves in Fig. 4. We can see that the four lobes of Imσ are now generated by increased strength of the inhomogeneity parameter D. Other phenomena are similar to those in Fig. 4.

To conclude this section, we can say that the behaviour of Imσ and $\cos\gamma$ is often rather complicated. Complexity increases with decreasing dissipation or with increasing $|D|$.

4 PLANE WAVES IN GENERAL VISCOELASTIC ANISOTROPIC MEDIA

In the preceding sections we considered the case of *SH* waves propagating in a symmetry plane of a viscoelastic anisotropic medium, which allows derivation of explicit analytical formulae and their simple analysis. In this section we present and discuss results obtained by numerical solution of eq. (3). In this way, we can investigate homogeneous and inhomogeneous plane waves propagating in arbitrary isotropic or anisotropic, perfectly elastic or anelastic media. We concentrate on inhomogeneous and homogeneous plane waves propagating in a cracked porous/permeable medium of hexagonal symmetry whose moduli were obtained by Jakobsen *et al.* (2003).

A matrix material of quartz is containing two sets of communicating pores. The first set consists of spherical pores; the second set consists of (randomly oriented) flat pores. In addition, the model includes a relatively high concentration of flat cracks that are nearly fully aligned (for more details see Jakobsen *et al.* 2003, p. 231). We choose the model corresponding to the frequency of approximately 35 Hz shown in their Fig. 2. For simplicity, we consider a density of 1000 kg m^{-3}. The matrix of complex-valued, density-normalized viscoelastic moduli of hexagonal symmetry with vertical axis of symmetry, measured in (km^2 s^{-2}) then reads:

$$\mathbf{A} = \mathbf{A}_1 - \mathrm{i}\mathbf{A}_2, \tag{14}$$

where

$$\mathbf{A}_1 = \begin{pmatrix} 46.631 & 5.983 & 4.278 & 0. & 0. & 0. \\ & 46.631 & 4.278 & 0. & 0. & 0. \\ & & 19.931 & 0. & 0. & 0. \\ & & & 13.444 & 0. & 0. \\ & & & & 13.444 & 0. \\ & & & & & 20.324 \end{pmatrix}$$

and

$$\mathbf{A}_2 = \begin{pmatrix} 0.033 & 0.022 & 0.156 & 0. & 0. & 0. \\ & 0.033 & 0.156 & 0. & 0. & 0. \\ & & 1.312 & 0. & 0. & 0. \\ & & & 0.055 & 0. & 0. \\ & & & & 0.055 & 0. \\ & & & & & 0.005 \end{pmatrix}.$$

For the above set of moduli, we calculate phase velocities $\mathcal{C}$, attenuation angle γ or its cosine, the quantity Imσ, the attenuation $|\mathbf{A}|$ and particle motion diagrams of the P wave and of two S waves. We first study the listed parameters as functions of the inhomogeneity parameter D, with the propagation angle i fixed, then as functions of propagation angle i with D fixed.

4.1 Plane waves in general anisotropic viscoelastic media: variations with D

In Fig. 6, we can see the variation of the phase velocity, of Imσ, of the attenuation $|\mathbf{A}|$ and of the attenuation angle γ in the plane of symmetry Σ^S of the model of the viscoelastic anisotropic medium (14). The propagation–attenuation plane $\Sigma^{\|}$ coincides again with the symmetry plane Σ^S. The propagation angle is fixed, $i = 45^\circ$, and the inhomogeneity parameter D varies from -0.2 to 0.2. The red colour corresponds to the fastest wave. According to its polarization, it is the P wave. The black colour corresponds to the faster of the S waves. It has SH-wave polarization. Finally the blue colour is reserved for the slowest wave, which has the SV-wave polarization. We can see that the phenomena observed in Figs 2 and 3, devoted to SH waves, can also be observed on the remaining waves.

(1) The *lack of symmetry* with respect to $D = 0$ is most pronounced in the plot of Imσ and of the attenuation angle γ. But it can be observed in all presented quantities for all waves.

(2) Thorough inspection reveals that the maxima of the *phase velocities* of all three waves are shifted slightly towards negative values of D. Thus, the homogeneous waves ($D = 0$) do not propagate with maximum phase velocities as is the case in isotropic media.

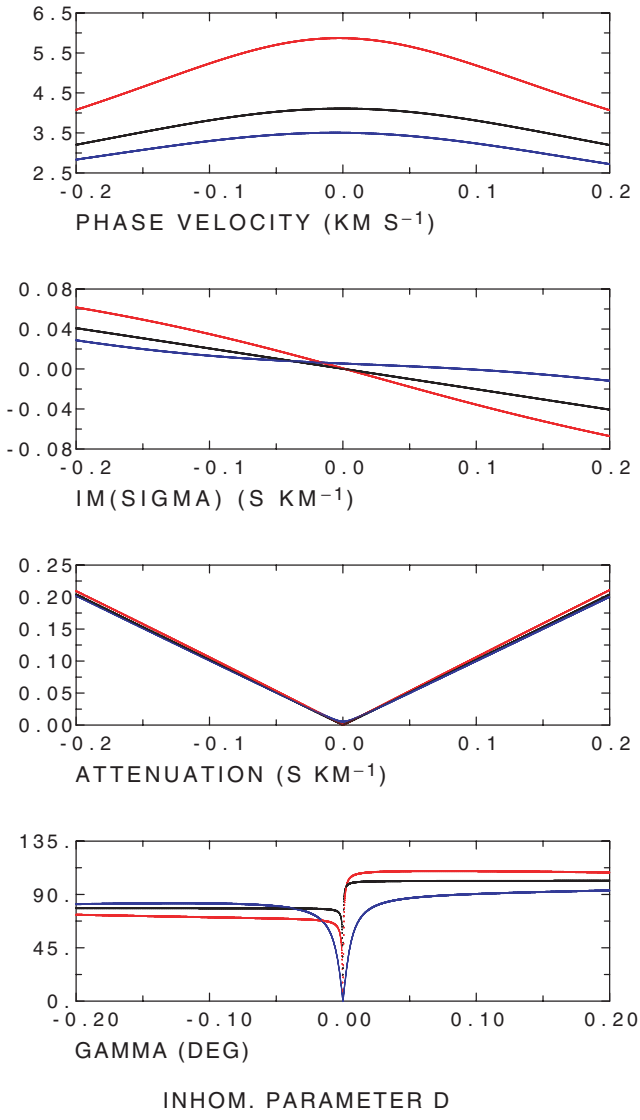

Figure 6. Variations with D of the phase velocity $\mathcal{C}$, Imσ, the attenuation $|\mathbf{A}|$ and the attenuation angle γ of plane waves in a plane of symmetry of the medium (14): red, the fastest wave (P wave); black, intermediate wave (SH wave); blue, the slowest wave (SV wave). The propagation angle $i = 45^\circ$.

They would if we had chosen the propagation angle i along the axis of symmetry or perpendicular to it.

(3) We can see that behaviour of Imσ, which controls exponential decay (growth) of amplitudes along the direction of propagation $\mathbf{N}$, is very similar to that of SH waves in Fig. 2. Variation with D is again nearly linear, thus linearized formulae could be used for its approximation. The slope of the curves differs, being greatest for the fastest wave and smallest for the slowest wave. Each wave has different value of D_0, for which Im$\sigma = 0$. For $D > D_0$ each wave attains negative values of Imσ, which means that the phenomenon of amplitudes of inhomogeneous plane waves growing in the direction of propagation, discussed in Section 3.2 for SH waves, holds for all three waves propagating in viscoelastic anisotropic media.

(4) Although the model used in this section differs considerably from the model (11) used for the SH waves, qualitative and quantitative behaviour of the *attenuation* is very similar. More pronounced differences can be found only for very small values of D. As in the case of SH waves, there is a shift of minima of individual waves

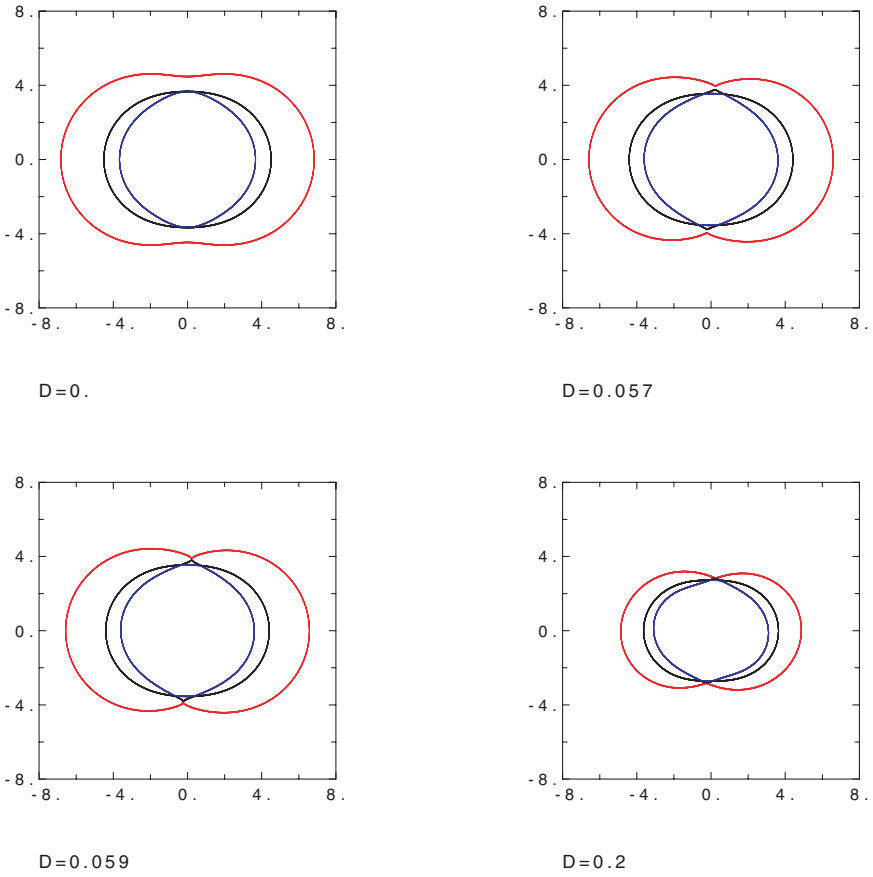

Figure 7. Polar diagrams of the phase velocity $\mathcal{C}$ (km s $^{-1}$) in a plane of symmetry of the medium (14) for $D = 0$ (homogeneous wave), 0.057, 0.059 and 0.2: red, the fastest wave (P wave); black, intermediate wave; blue, the slowest wave. Note that SV wave is slowest in most directions but intermediate in the vertical direction for $D \geq 0.057$.

from the value $D = 0$ (homogeneous wave), but the shift is very small. The minimum values of the attenuation are nearly zero.

(5) The *attenuation angle* γ is zero for $D = 0$ but otherwise the behaviour of the curves for individual waves is strongly non-symmetric. The lack of symmetry increases with increase in the phase velocity of the wave. A similar observation also holds for the speed of variation of γ in the vicinity of $D = 0$. As in the case of SH waves, we can see that the boundary attenuation angles γ^* for $D \to -\infty$ and $D \to \infty$ differ. For $D \to -\infty$, γ^* is less than 90°, for $D \to \infty$, it exceeds 90°.

Similar phenomena as above could also be observed for other angles of propagation i. Only their intensity would vary.

4.2 Plane waves in general anisotropic viscoelastic media: variations with the propagation angle *i*

Now we study properties of the P and S waves as functions of the propagation angle i for several selected values of the inhomogeneity parameter D in the symmetry plane Σ^S of the model of the viscoelastic anisotropic medium (14). Again, the propagation–attenuation plane coincides with the symmetry plane. As before, the red colour indicates the fastest, the black colour the intermediate and blue colour the slowest wave. We present polar plots, in which $i = 0°$ is upwards and $i = 90°$ to the right (see eq. 4). In all cases absolute values of the studied quantities are shown, although some of them like $\cos(\gamma)$ or $\mathrm{Im}\sigma$ may change their sign.

In Fig. 7, *phase velocity* polar graphs for four values of the inhomogeneity parameter D, $D = 0$ (homogeneous wave), $D = 0.057$, $D = 0.059$ and $D = 0.2$ are shown. For $D = 0$, the phase velocities are symmetrical with respect to the vertical axis. The highest (red) phase-velocity surface is separated from the remaining velocities and corresponds to the P wave. The higher of the remaining velocities corresponds to the SH wave (see the particle motion diagram in Fig. 11), the slower to the SV wave. Both S-wave phase velocities touch on the vertical axis. For increasing values of D, the P-wave and SV-wave phase velocity curves deform ($D = 0.057$) close to the vertical axis and approach each other. The SV-wave phase velocity curve intersects the SH-wave curve. Therefore, the relevant part of the SV-wave phase velocity is black in Fig. 7. The phase velocities are no longer symmetrical with respect to the vertical axis. With increasing D, the curves of the P- and SV-wave velocities come into contact, i.e. for the corresponding propagation angle i (which is non-zero), the P and SV waves propagate with the same phase velocity. With further increase of D, the phase velocities decrease (they become zero for $|D| \to \infty$) and all three phase-velocity curves become nearly indistinguishable. Let us emphasize that the individual plots in Fig. 7 show phase velocities corresponding to the slowness vector (1) with a selected *constant inhomogeneity parameter D*. Except for $D = 0$ (which corresponds to $\gamma = 0°$ or 180°, see eq. 7), the plots corresponding to a slowness vector with a *fixed attenuation angle* γ would be different.

In viscoelastic or perfectly elastic *isotropic* media, the relevant curves of phase velocities of both P and S waves would be circular.

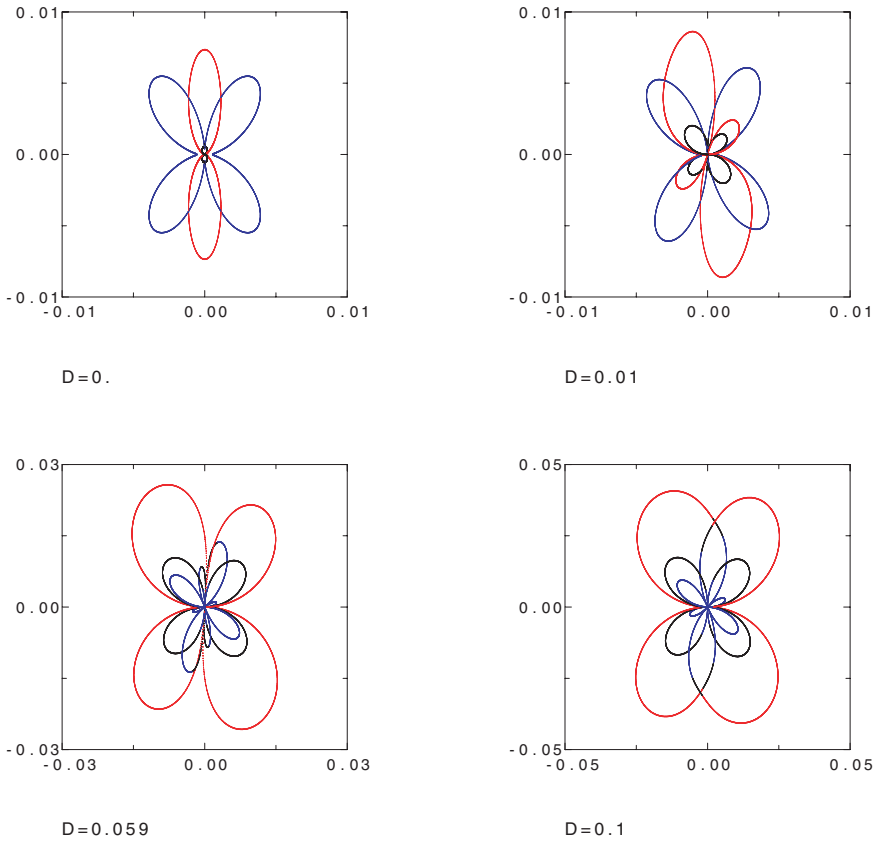

Figure 8. Polar diagrams of $|\mathrm{Im}\sigma|$ (s km^{-1}) in a plane of symmetry of the medium (14) for $D = 0$ (homogeneous wave), 0.01, 0.059 and 0.1. The colours are as in Fig. 7.

Fig. 8 shows the polar plots of the absolute values of the *quantity* $\mathrm{Im}\sigma$ for four values of D, $D = 0$, $D = 0.01$, $D = 0.059$ and $D = 0.1$. We can see that the plots have quite a complicated character, with several lobes. For the case of homogeneous waves ($D = 0$), the plots are symmetrical with respect to the vertical and horizontal axes. The *P* and *SH* waves have two lobes extending along the vertical axis. In the horizontal direction, the values of $\mathrm{Im}\sigma$ are effectively zero. The *SV* wave (blue) has four lobes. All the values of $\mathrm{Im}\sigma$ for $D = 0$ are positive. With increasing D, the symmetrical nature of the plots with respect to the vertical disappears and the plots become more complicated. For $D = 0.01$, each of the three waves has four lobes. The lobes of the *SV* wave are related again to positive values of $\mathrm{Im}\sigma$. The new (smaller) lobes of the *P* and *SH* waves, however, are related to negative values. This means that in the corresponding directions, amplitudes of the *P* and *SH* waves increase in the direction of propagation. The plot for $D = 0.059$ corresponds to the value of D for which the *P*- and *SV*-wave phase velocity curves come into contact (see Fig. 7). We can see that the number of lobes of the *S* waves is again increased. The number of lobes of *P* and *SH* waves is four as for $D = 0.01$. The number of lobes of the *SV* wave is increased to eight! The increased number of lobes is related to the intersection of the two *S*-wave phase velocity sheets. There are already eight lobes for $D = 0.057$. Also note the increase in the absolute value of $\mathrm{Im}\sigma$. A closer inspection reveals that some of the lobes abruptly change colour from blue to black and vice versa. This is a consequence of the fact that the colours do not correspond to wave modes defined by their polarization. When we increase D to $D = 0.1$, there are again four lobes for each wave. We can, however, observe abrupt changes of all three colours. This is because the phase velocities of all the three waves are interconnected (see Fig. 7). Some lobes of each wave are related to negative values.

In a viscoelastic *isotropic* medium, the curve of $\mathrm{Im}\sigma$ would be circular for each wave. In an elastic isotropic medium, it would reduce to a point.

In Fig. 9, behaviour of the *attenuation* $|\mathbf{A}|$ is illustrated in plots corresponding to $D = 0$, $D = 0.001$, $D = 0.005$ and $D = 0.01$. For small values of D, behaviour of the attenuation is very similar to that of $\mathrm{Im}\sigma$. This is obvious from eqs (7). For $D = 0$, $|\mathbf{A}| = |\mathrm{Im}\sigma|$. For small values of D, attenuation is more anisotropic than phase velocity. This is in agreement with observations made by Hosten *et al.* (1987). As in Fig. 9, Hosten *et al.* (1987) also observed directions in which, in contrast to isotropic media, *P*-wave attenuation was larger than *S*-wave attenuation. In our case, such a direction is the direction along the axis of symmetry. In the direction perpendicular to the axis of symmetry, the attenuation is small and nearly equal for all waves. Anisotropy of the attenuation of all three waves decreases considerably with increasing D while $|\mathbf{A}|$ itself increases. Attenuation of the *SH* wave (black) has, except for the case of a homogeneous wave, a nearly circular character for any non-zero value of D. In the horizontal direction, the attenuation of all three waves is equal for non-zero D.

For viscoelastic isotropic media, the curves in Fig. 9 would be circular. For perfectly elastic isotropic media, the radius of the circles would be $|D|$.

The behaviour of the *attenuation angle* γ is very interesting, specifically of the absolute value of $\cos\gamma$, which is shown in Fig. 10. For $D = 0$, cosines of the attenuation angles γ of *P* and *S* waves are unity, i.e. $\gamma = 0$, which indicates homogeneous waves. For

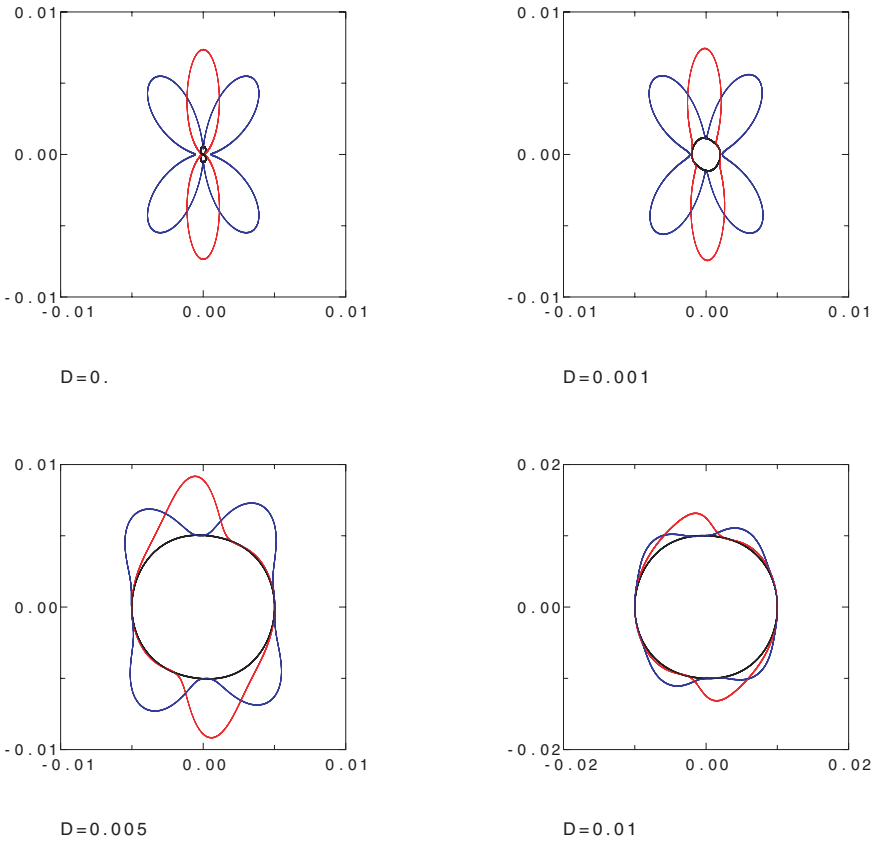

Figure 9. Polar diagrams of the attenuation $|\mathbf{A}|$ (s km $^{-1}$) in a plane of symmetry of the medium (14) for $D = 0$ (homogeneous wave), 0.001, 0.005 and 0.01. The colours are as in Fig. 7.

$D = 0.0001$, the cosine corresponding to the *SV* wave remains nearly unity. The diagram is only slightly reduced in the horizontal direction. Cosines of the *P* and *SH* waves are unity only in the vicinity of the vertical direction. They are both minimum in the horizontal direction. For $D = 0.001$, the cosine of the *P* wave has four lobes. Two big lobes are along the vertical axis and correspond to positive values of $\cos\gamma$, i.e. to values of γ less than 90°. Two very small hardly visible lobes correspond to negative values of $\cos\gamma$, i.e. to values of γ greater than 90°. The *SV* wave also has a four-lobe character with γ always less than 90°. The *SH*-wave curves consist of two lobes only with nearly vertical orientation and significantly reduced size, which means that the attenuation angle γ is for all directions of propagation considerably different from zero. This is not true for *P* and *SV* waves, for which there are directions in which the angle γ is zero or close to zero. This situation changes considerably when *D* is further increased. For $D = 0.01$, the angles γ of all waves differ considerably from zero. The curves of $\cos\gamma$ of all waves now have a four-lobed character. The smaller lobes of *P* and *SH* waves have negative values, and all lobes of the *SV* wave have positive values. For $D \geq 1$, the plots of cosines of the attenuation angle become insensitive to the variation of *D*. This means that the plot for $D = 1$ can be taken as an approximation of the plot of $\cos\gamma^*$, i.e. of the cosine of the boundary attenuation angle. The values of γ greater than γ^* correspond to the forbidden directions discussed in Section 5. Note that γ^* is generally different from 90° as in Figs 2 and 3. Since values of $\cos\gamma$ are negative in the bottom left–upper right direction, the angles γ^* are larger than 90° in these directions. For the bottom right–upper left direction, the angles γ^* are less than 90°.

Let us note that in viscoelastic *isotropic* media, all curves for *P* and *S* waves would be circular and would always correspond to positive values of $\cos\gamma$, indicating that the attenuation angle is directionally independent and $0° < \gamma < 90°$. The angle γ would become 90° for perfectly elastic isotropic medium.

The behaviour of *polarization* of all the three waves discussed is shown in Fig. 11. The polarization vectors are calculated from eq. (2). The vectors $\mathbf{U}$ are normalized so that $U_i U_i^* = 1$. Particle motion diagrams show several interesting phenomena. We can see that even for $D = 0$, i.e. for homogeneous waves, the particle motion of *P* and *SV* waves is elliptical in all directions except specific ones. For the directions along and perpendicular to the axis of symmetry of the medium (14), the polarization of homogeneous waves is linear. In this respect, it is interesting to note that for $D > 0$, i.e. for inhomogeneous waves, the strongest elliptical polarization of *P* and *SV* waves can be observed along the vertical. Since we study plane waves in the symmetry plane of the medium (14), *SH*-wave polarization is always linear, no matter which value of *D* is considered, and perpendicular to the plane of the plots. We can also see that with increasing *D* it becomes more and more difficult (and for *D* greater than shown in Fig. 11 even impossible) to distinguish *P* and *SV* waves according to their polarization. Another interesting phenomenon is the black ellipses along the vertical for $D = 0.05$ and 0.1. They indicate that the *SV* wave is no longer the slowest wave in this direction. The slowest is now the *SH* wave (see Fig. 7). Finally we can see that increase of value of *D* destroys the symmetry of the plots with respect to the vertical.

So far we studied behaviour of various characteristics of plane waves propagating so that the propagation–attenuation plane $\Sigma^{\|}$

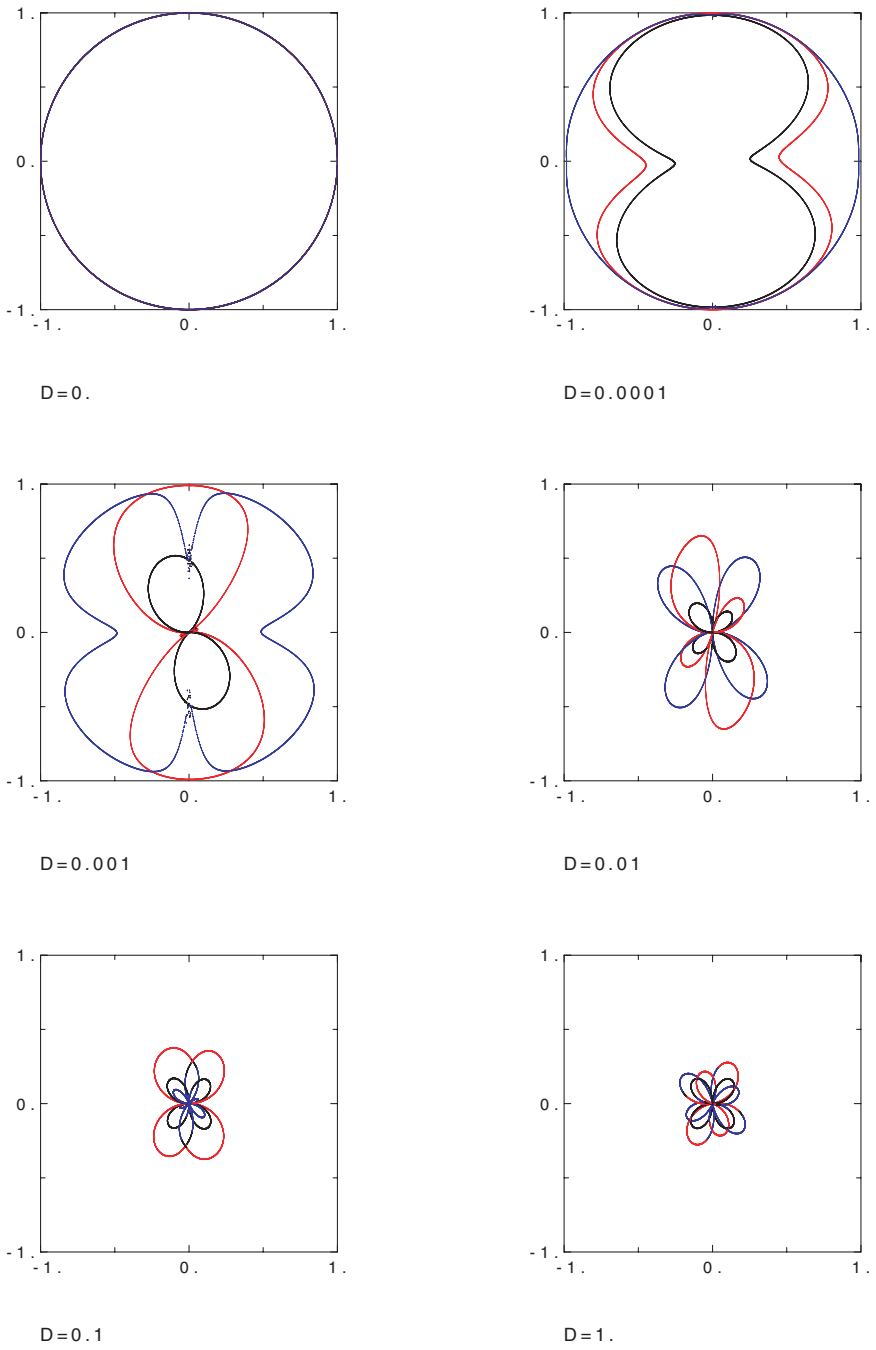

Figure 10. Polar diagrams of $|\cos\gamma|$ in a plane of symmetry of the medium (14) for $D = 0$ (homogeneous wave), 0.0001, 0.001, 0.01, 0.1 and 1. The colours are as in Fig. 7.

coincided with the symmetry plane Σ^S of the viscoelastic anisotropic media. There is no problem making similar studies in planes $\Sigma^{\|}$, different from the symmetry planes. We would find that most of the above observed phenomena are observable in these cases as well, the plots being only slightly more complicated. As an example, we show the behaviour of polarization in the vertical plane $\Sigma^{\|}$ through the model (14) rotated first by 45° around the x_3-axis and then again by 45° around the new x_2-axis. Fig. 12 shows a projection of the particle motion into the propagation–attenuation plane $\Sigma^{\|}$. Because $\Sigma^{\|}$ no longer coincides with the symmetry plane, we can observe particle motion of all three waves in Fig. 12. Note that for $D \geq 0.05$ it becomes difficult to distinguish the two S waves, at least in the presented plots.

5 EXPLANATION OF FORBIDDEN DIRECTIONS IN DIRECTIONAL SPECIFICATION

The mixed specification (1) of the slowness vector offers a simple explanation of the phenomenon of *forbidden directions*, first discovered in the pioneering works of Krebes & Le (1994) and Carcione & Cavallini (1995, 1997). These authors used the

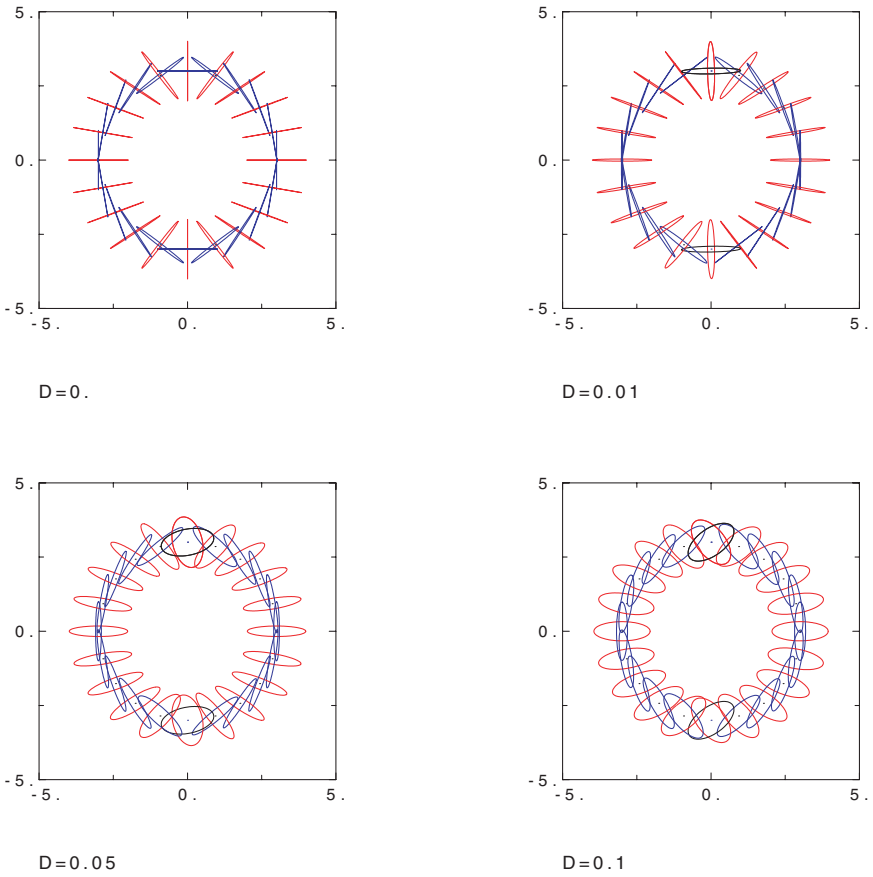

Figure 11. Polar diagrams of the polarization in a plane of symmetry of the medium (14) for $D = 0$ (homogeneous wave), 0.01, 0.05 and 0.1. The colours are as in Fig. 7. *SH*-wave polarization is perpendicular to the plots.

directional specification of the slowness vector, and specified the slowness vector by the propagation angle i and the attenuation angle γ. For γ fixed, they obtained negative values of $\mathcal{C}^2$ for certain propagation angles i. This result was interpreted in such a way that these propagation directions i are forbidden for inhomogeneous plane waves with γ given or larger. The above result indicates that the specification of the slowness vector by fixed attenuation angle γ is connected with certain problems. Indeed, use of the mixed specification by Červený & Pšenčík (2005) and in this paper showed that γ must always be less than the boundary attenuation angle γ^*, which means that γ cannot be chosen arbitrarily. The determination of γ^* within the directional specification of the slowness vector is, however, very difficult if not impossible. For this reason, it is more reasonable to use the inhomogeneity parameter D, which is subjected to no restrictions for the specification of the slowness vector.

For simplicity, let us illustrate the problem of forbidden directions with the case of inhomogeneous *SH* plane waves propagating in the model (11). The model resembles closely the model used by Carcione & Cavallini (1995) to study forbidden directions. Carcione & Cavallini (1995) showed that, for fixed $\gamma > 64^\circ$, two regions of forbidden directions are formed close to propagation angles $i = 135^\circ$ and 315°. Let us have a look at this problem in the i, γ and i, D domains.

The upper plot of Fig. 13 shows squares of the phase velocities $\mathcal{C}^2$ for four fixed values of γ, the middle and bottom plots show the phase velocities $\mathcal{C}$ and the attenuation angle γ for four fixed values of D, all as functions of the propagation angle i. The curves of $\mathcal{C}^2$ in the upper plot are parametrized by the following values of the attenuation angle γ: $\gamma = 25^\circ$ (black), $\gamma = 58^\circ$ (red), $\gamma = 60^\circ$ (green) and $\gamma = 62^\circ$ (blue). This plot corresponds qualitatively to Fig. 4.6 of Carcione (2001). We can see that for $\gamma = 25^\circ$ and 58°, the curves attain positive values of $\mathcal{C}^2$ for any propagation angle i. For $\gamma = 60^\circ$ and 62°, however, we can observe that $\mathcal{C}^2$ attains negative values for some angles i. These represent the forbidden directions.

In the middle plot, the phase velocities $\mathcal{C}$ are parametrized by the inhomogeneity parameters D: $D = 10$ (black), $D = 1$ (red), $D = 0.03$ (green) and $D = 0.01$ (blue). The green and blue curves practically coincide. The bottom plot shows behaviour of the attenuation angles γ corresponding to the mentioned fixed values of D. For D greater than, say, 1, the values of γ practically do not change with increasing D. Consequently, the curves of γ for $D = 1$ and $D = 10$ practically coincide, and can be considered as the boundary attenuation angle γ^*. All curves in the middle and bottom plots are smooth and simple; they do not display any negative values of $\mathcal{C}$.

Let us have a closer look at the boundary attenuation angle γ^*, represented by the uppermost curve in the bottom plot of Fig. 13. We can see that the boundary attenuation angle γ^* depends strongly on the propagation angle i; it has two minima $\gamma^*_{\min} = 60.5^\circ$ at $i = 135^\circ$ and $i = 315^\circ$, and two maxima $\gamma^*_{\max} = 119.4^\circ$ at $i = 15^\circ$ and $i = 195^\circ$. For a given propagation angle i, the inhomogeneous plane waves with an attenuation angle γ greater than the boundary attenuation angle γ^* **do not exist**. Thus, for any fixed $\gamma < \gamma^*_{\min}$, the inhomogeneous plane waves exist for any propagation angle i. For $\gamma^*_{\min} < \gamma < \gamma^*_{\max}$, two forbidden regions are developed in the

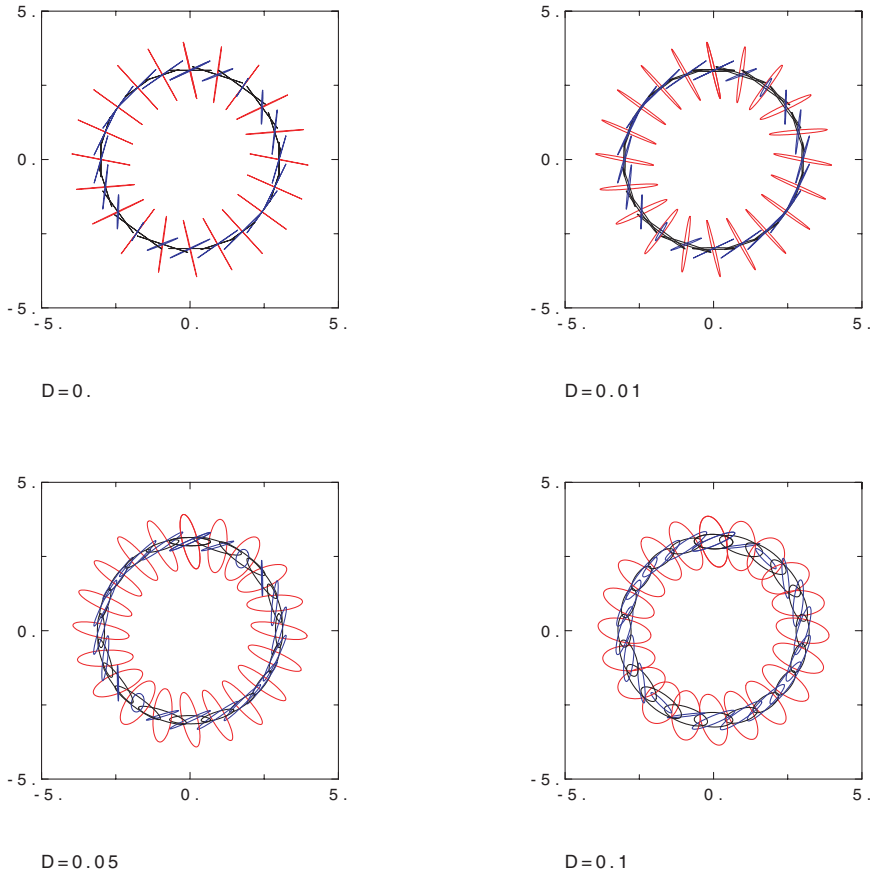

Figure 12. Polar diagrams of the polarization in a rotated model of the medium (14) for $D = 0$ (homogeneous wave), 0.01, 0.05 and 0.1. The colours are as in Fig. 7.

i, γ domain. In our case, the first is concentrated around $i = 135^\circ$, and the second around 315°. Finally, for $\gamma > \gamma^*_{\max}$, inhomogeneous plane waves do not exist for any propagation angle i.

Let us consider, as an example, a fixed attenuation angle $\gamma = 62^\circ$ (see the horizontal black line in the bottom plot of Fig. 13). Then the boundaries of the forbidden regions (intersections of the uppermost curve corresponding to γ^* with the horizontal black line) in the bottom plot correspond exactly to the intersections of the blue curve ($\gamma = 62^\circ$) with zero in the upper plot.

6 CONCLUSION

The mixed specification of the slowness vector, based on the use of unit vectors **n** and **m**, and the inhomogeneity parameter D, can be used to study homogeneous or inhomogeneous waves propagating in elastic or viscoelastic, isotropic or anisotropic media. Problems with non-physical results related to forbidden directions, which exist in the directional specification, do not exist in the mixed specification. On the contrary, the mixed specification offers a simple way of calculation of the boundary attenuation angles specifying which attenuation angles are allowed and which are not. In case of *SH* plane waves, the mixed specification yields explicit analytical expressions, which can be directly analysed.

The results obtained with the mixed specification show several phenomena unknown from studies of wave propagation in perfectly elastic isotropic or anisotropic and viscoelastic isotropic media. Most of them have been predicted by analysis of simple analytical formulae describing plane wave propagation in a symmetry plane of a viscoelastic anisotropic medium in Červený & Pšenčík (2005). For example, it was shown that in contrast to the wave propagation in viscoelastic isotropic media, the maximum phase velocity in a given direction might not be associated with the homogeneous wave. Similarly, the minimum attenuation might not be associated with the relevant homogeneous wave. The amplitudes of inhomogeneous waves may increase exponentially in the direction of propagation. Anisotropy of attenuation is often greater than anisotropy of velocities. Except for some special directions, polarization of all waves is, in general, elliptical.

As in Červený & Pšenčík (2005), we considered plane waves throughout the paper. We consider such study to be a necessary step before solving problems of propagation of non-planar waves in complex media.

ACKNOWLEDGMENTS

The authors are greatly indebted to Luděk Klimeš for helpful suggestions and valuable discussions and to José Carcione and Fabio Cavallini for their critical review. Thanks to Morten Jakobsen for providing the data for numerical examples. The research has been supported by the Consortium Project ‘Seismic Waves in Complex 3-D Structures’, by the research projects 205/04/1104 and 205/05/2182 of the Grant Agency of the Czech Republic, by the research project A3012309 of the Grant Agency of the Academy of Sciences of the Czech Republic, by the Ministry of Education

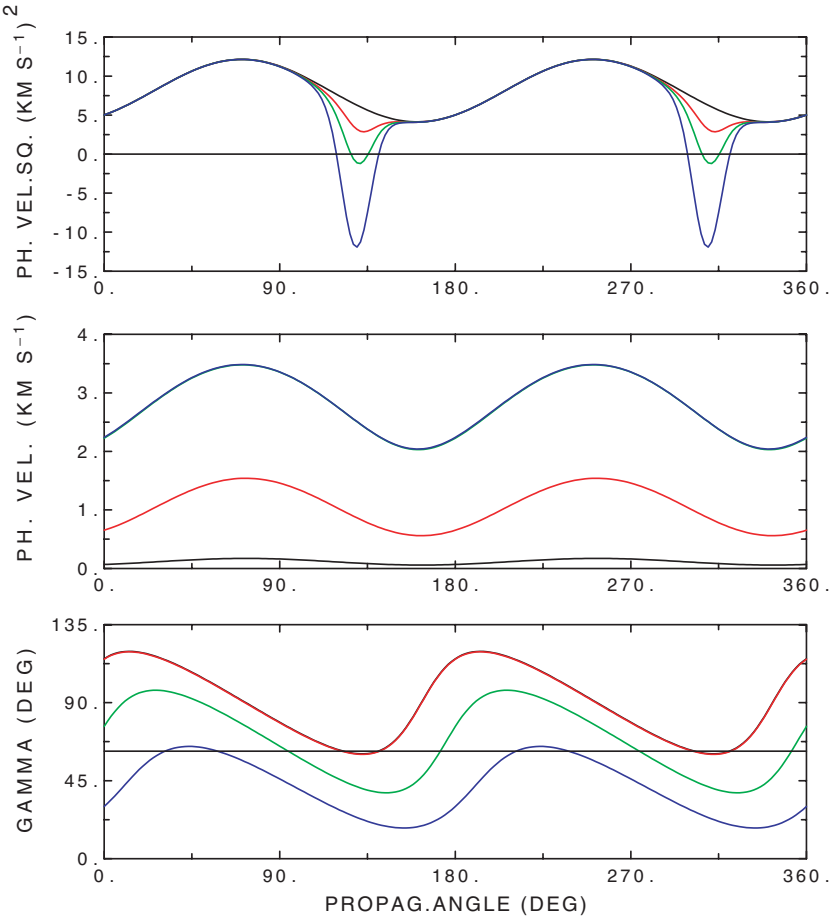

Figure 13. Explanation of the forbidden directions. Inhomogeneous *SH* plane waves in a plane of symmetry of the anisotropic medium (11). Dependence of C^2, C and γ on the propagation angle i. The upper plot of C^2 parametrized by γ: $\gamma = 25^\circ$ (black), $\gamma = 58^\circ$ (red), $\gamma = 60^\circ$ (green) and $\gamma = 62^\circ$ (blue). Note that green and blue curves intersect zero, thus defining forbidden directions. The middle and bottom plots of C and γ parametrized by D: $D = 10$ (black), $D = 1$ (red), $D = 0.03$ (green) and $D = 0.01$ (blue). The curves for γ in the bottom plot coincide for $D \geq 1$ (see the uppermost red curve for $D = 1$, which coincides with the black one for $D = 10$). Coinciding curves thus represent the boundary attenuation angle γ^*. For $\gamma = 62^\circ$ (black horizontal line in the bottom plot), inhomogeneous plane waves cannot exist for i close to 130° and 310°, where $\gamma > \gamma^*$, i.e. the horizontal line intersects the uppermost curve. For more details see text.

of the Czech Republic under research project MSM113200004, and by the Academy of Sciences within research projects Z3012916 and K3012103. Part of this work was done during the IP's stay at the University of Hamburg sponsored by DFG project TSE 17/5/02 within Ga 350/10-1.

REFERENCES

Aki, K. & Richards, P., 1980. *Quantitative Seismology. Theory and Methods,* Freeman, San Francisco, CA.

Buchen, P.W., 1971. Plane waves in linear viscoelastic media, *Geophys. J.R. astr. Soc.,* **23,** 531–542.

Borcherdt, R.D., 1973. Energy and plane waves in linear viscoelastic media, *J. geophys. Res.,* **78,** 2442–2453.

Borcherdt, R.D., 1977. Reflection and transmission of type II S waves in elastic and anelastic media, *Bull. seism. Soc. Am.,* **67,** 43–67.

Borcherdt, R.D. & Wennerberg, L., 1985. General P, type-I S and type-II S waves in anelastic solids: inhomogeneous wave fields in low-loss solids, *Bull. seism. Soc. Am.,* **75,** 1729–1763.

Borcherdt, R.D., Glassmoyer, G. & Wennerberg, L., 1986. Influence of welded boundaries in anelastic media on energy flux, and characteristics of P, S-I and S-II waves: observational evidence for inhomogeneous body waves in low-loss solids, *J. geophys. Res.,* **91,** 11 503–11 518.

Brokešová, J. & Červený, V., 1998. Inhomogeneous plane waves in dissipative isotropic and anisotropic media. Reflection/transmission coefficients, in, *Seismic Waves in Complex 3-D Structures,* Report 7, pp. 57–146, Faculty of Mathematics and Physics, Department of Geophysics, Charles University, Prague (available online at http://sw3d.mff.cuni.cz).

Carcione, J.M., 1993. Seismic modelling in viscoelastic media, *Geophysics,* **58,** 110–120.

Carcione, J.M., 2001. *Wave Fields in Real Media: Wave Propagation in Anisotropic, Anelastic and Porous Media,* Pergamon, Amsterdam.

Carcione, J.M. & Cavallini, F., 1995. Forbidden directions for inhomogeneous pure shear waves in dissipative anisotropic media, *Geophysics,* **60,** 522–530.

Carcione, J.M. & Cavallini, F., 1997. Forbidden directions for TM waves in anisotropic conducting media, *IEEE Trans. Antennas Propag.,* **45,** 133–139.

Caviglia, G. & Morro, A., 1992. *Inhomogeneous Waves in Solids and Fluids,* World Scientific, Singapore.

Červený, V., 2004. Inhomogeneous harmonic plane waves in viscoelastic anisotropic media., *Stud. Geophys. Geod.,* **48,** 167–186.

Červený, V. & Pšenčík, I., 2005. Slowness vectors in viscoelastic anisotropic media—I. Theory, *Geophys. J. Int.,* **161,** 197–212 (this issue).

Fedorov, F.I., 1968. *Theory of Elastic Waves in Crystals,* Plenum, New York.

Hosten, B., Deschamps, M. & Tittmann, B.R., 1987. Inhomogeneous wave generation and propagation in lossy anisotropic solids. Applications to the characterization of viscoelastic composite materials, *J. acoust. Soc. Am.,* **82,** 1763–1770.

Jakobsen, M., Johansen, T.A. & McCann, C., 2003. The acoustic signature of fluid flow in complex porous media, *J. appl. Geophys.,* **54,** 219–246.

Krebes, E.S., 1983. The viscoelastic reflection/transmission problem: two special cases, *Bull. seism. Soc. Am.,* **73,** 1673–1683.

Krebes, E.S. & Le, L.H.T., 1994. Inhomogeneous plane waves and cylindrical waves in anisotropic anelastic media., *J. geophys. Res.,* **99**(B12), 23 899–23 919.

Press, W.H., Flannery, B.P., Teukolsky, S.A. & Vetterling, W.T., 1986. *Numerical Recipes,* Cambridge University Press, Cambridge.

Richards, P.G., 1984. On wavefronts and interfaces in anelastic media, *Bull. seism. Soc. Am.,* **74,** 2157–2165.